British Journal of Pharmacology

British Journal of Pharmacology (2016) **173** 3327–3341 3327

RESEARCH PAPER

Selective targeting of CREB-binding protein/β-catenin inhibits growth of and extracellular matrix remodelling by airway smooth muscle

Correspondence Tim Koopmans, Department of Molecular Pharmacology, University of Groningen, Antonius Deusinglaan 1, 9713 AV, Groningen, The Netherlands. E-mail: t.koopmans@rug.nl

Received 6 May 2016; **Revised** 17 August 2016; **Accepted** 7 September 2016

Tim Koopmans[1,2], Stijn Crutzen[1,2], Mark H Menzen[1,2], Andrew J Halayko[3], Tillie-Louise Hackett[4], Darryl A Knight[4,5,6] and Reinoud Gosens[1,2]

[1]Department of Molecular Pharmacology, University of Groningen, Groningen, The Netherlands, [2]Groningen Research Institute for Asthma and COPD (GRIAC), University of Groningen, Groningen, The Netherlands, [3]Department of Physiology and Pathophysiology, University of Manitoba, Winnipeg, MB, Canada, [4]Department of Anesthesiology, Pharmacology & Therapeutics, University of British Columbia, Vancouver, BC, Canada, [5]School of Biomedical Sciences and Pharmacy, The University of Newcastle, Callaghan, NSW, Australia, and [6]Asthma, Allergy and Infection Research Cluster, Hunter Medical Research Institute, New Lambton Heights, NSW, Australia

BACKGROUND AND PURPOSE

Asthma is a heterogeneous chronic inflammatory disease, characterized by the development of structural changes (airway remodelling). β-catenin, a transcriptional co-activator, is fundamentally involved in airway smooth muscle growth and may be a potential target in the treatment of airway smooth muscle remodelling.

EXPERIMENTAL APPROACH

We assessed the ability of small-molecule compounds that selectively target β-catenin breakdown or its interactions with transcriptional co-activators to inhibit airway smooth muscle remodelling *in vitro* and *in vivo*.

KEY RESULTS

ICG-001, a small-molecule compound that inhibits the β-catenin/CREB-binding protein (CBP) interaction, strongly and dose-dependently inhibited serum-induced smooth muscle growth and TGFβ1-induced production of extracellular matrix components *in vitro*. Inhibition of β-catenin/p300 interactions using IQ-1 or inhibition of tankyrase 1/2 using XAV-939 had considerably less effect. In a mouse model of allergic asthma, β-catenin expression in the smooth muscle layer was found to be unaltered in control versus ovalbumin-treated animals, a pattern that was found to be similar in smooth muscle within biopsies taken from asthmatic and non-asthmatic donors. However, β-catenin target gene expression was highly increased in response to ovalbumin; this effect was prevented by topical treatment with ICG-001. Interestingly, ICG-001 dose-dependently reduced airway smooth thickness after repeated ovalbumin challenge, but had no effect on the deposition of collagen around the airways, mucus secretion or eosinophil infiltration.

CONCLUSIONS AND IMPLICATIONS

Together, our findings highlight the importance of β-catenin/CBP signalling in the airways and suggest ICG-001 may be a new therapeutic approach to treat airway smooth muscle remodelling in asthma.

Abbreviations

ASM, airway smooth muscle; Axin, axis inhibition protein; CBP, CREB-binding protein; ECM, extracellular matrix; GSK, glycogen synthase kinase; OVA, ovalbumin; PAS, periodic acid Schiff; PDGF, platelet-derived growth factor; TCF, T-cell factor; WISP, WNT1 inducible signalling pathway protein; WNT, wingless-type and integrase 1; α-SMA, α-smooth muscle actin

DOI:10.1111/bph.13620

Tables of Links

TARGETS	
Other protein targets[a]	**Enzymes**[b]
CREB binding protein	GSK-3β
E1A binding protein p300	MMP
	PDGFRα
	Activin A receptor type 1 (ALK2)

LIGANDS
β-Catenin
PDGF AB
TGFβ1

These Tables list key protein targets and ligands in this article which are hyperlinked to corresponding entries in http://www.guidetopharmacology.org, the common portal for data from the IUPHAR/BPS Guide to PHARMACOLOGY (Southan *et al.*, 2016) and are permanently archived in the Concise Guide to PHARMACOLOGY 2015/16 ([a,b]Alexander *et al.*, 2015a,b).

Introduction

Asthma is a chronic inflammatory disease of the large and small airways, estimated to affect 235 million people worldwide (WHO, 2013). A cardinal feature of asthma is airway hyper-responsiveness, which is defined as the exaggerated bronchoconstriction response to specific and non-specific stimuli, in which the airway smooth muscle (ASM) is fundamentally involved. Airway hyper-responsiveness has a variable and persistent component. The variable component is dependent on chronic airway inflammation, involving a wide range of inflammatory cells, whereas the persistent component is dependent on the manifestation of structural changes, or airway remodelling (Meurs *et al.*, 2008). Airway remodelling encompasses increased ASM mass, mucous gland hypertrophy, angiogenesis, subepithelial fibrosis and epithelial changes including cell detachment and goblet cell hyperplasia.

Chronic inflammation has long been considered the primary cause of structural tissue changes. While there is much evidence to support this (Flood-Page *et al.*, 2003; Humbles *et al.*, 2004), an increasing amount of evidence suggests that airway remodelling already occurs early on in the natural pathogenesis of asthma, even before the onset of symptoms. Reticular basement membrane thickening (Cutz *et al.*, 1978; Cokuğraş *et al.*, 2001; Payne *et al.*, 2003), epithelial damage, vessel formation (Barbato *et al.*, 2006) and increased ASM thickness (Cutz *et al.*, 1978; Jenkins *et al.*, 2003; Regamey *et al.*, 2007) have all been described in young children with asthma. Moreover, many studies have been unable to demonstrate a relationship between airway inflammation or asthma duration on the one hand and severity of airway remodelling on the other (Hoshino *et al.*, 1998; Benayoun *et al.*, 2003; Payne *et al.*, 2003; James *et al.*, 2009), and clinical symptoms remain relatively constant with age (Horak *et al.*, 2003; Sears *et al.*, 2003). These findings challenge the paradigm that airway remodelling is a direct consequence of inflammation and suggest that the two may develop in parallel. Current asthma treatment is mainly focused on reducing inflammation and relaxing ASM, while no drug therapy exists that primarily targets airway remodelling.

β-catenin is a key component of adherens junctions that links family members of the transmembrane protein cadherin [N-cadherin in ASM (Gosens *et al.*, 2010)] to the cytoskeleton and is involved in cell–cell adhesion (McCrea and Gu, 2010). In addition, β-catenin is a critical effector of both wingless-type and integrase 1 (WNT)-dependent and independent signalling where it functions as a transcriptional co-activator. The central event for the induction of β-catenin signalling is the accumulation of β-catenin in the cytosol followed by its translocation to the nucleus. In the absence of extracellular signals, levels of β-catenin are being kept low by means of an axis inhibition protein (Axin)-adenomatous polyposis coli complex that captures β-catenin and subjects it to phosphorylation by glycogen synthase kinase (GSK)-3β and casein kinase (CK)-Iα, leading to its proteasomal degradation (Metcalfe and Bienz, 2011; Baarsma *et al.*, 2013). Conversely, when WNT ligands bind frizzled (FZD) receptors in association with LRP-5/6 co-receptors, the destruction complex is sequestered towards the membrane, effectively preventing β-catenin from GSK-3β-mediated phosphorylation, and allowing it to accumulate (Metcalfe and Bienz, 2011; Baarsma *et al.*, 2013). WNT-independent mechanisms also contribute to the stabilization of β-catenin via growth factors such as platelet-derived growth factor (PDGF) and TGFβ1 which regulate nuclear β-catenin accumulation through Akt and GSK-3β (Kumawat *et al.*, 2014). In the nucleus, β-catenin associates with a plethora of interaction partners, consequently leading to the transcriptional regulation of genes (Valenta *et al.*, 2012), many of which are involved in tissue repair and remodelling (Königshoff and Eickelberg, 2010). To assemble a transcriptional complex, β-catenin depends on the transcriptional co-activators CREB-binding protein (CBP) or its closely related homologue E1A-associated protein p300 (Hecht *et al.*, 2000; Takemaru and Moon, 2000). In smooth muscle, β-catenin plays a critical role in pro-mitogenic signalling, which has been shown *in vitro* (Nunes *et al.*, 2008; Gosens *et al.*, 2010) and *in vivo* (De Langhe *et al.*, 2008; Cohen *et al.*, 2009; Volckaert *et al.*, 2011). Moreover, TGFβ1-mediated production of extracellular matrix (ECM) proteins in ASM is dependent on β-catenin activation (Baarsma *et al.*, 2011). The roles of CBP and p300 in these processes have not been investigated yet.

Targeting β-catenin in ASM to inhibit airway remodelling may be an interesting new approach in the context of asthmatic airway remodelling. In this study, we sought to

evaluate the potential of pharmacological β-catenin inhibition on ASM proliferation and ECM production, using commercially available small-molecule compounds that selectively attenuate the nuclear functions of β-catenin. With this aim, we evaluated the efficacy of ICG-001, a compound that prevents the interaction of β-catenin with CBP, IQ-1, a compound that prevents the interaction of β-catenin with p300, and XAV-939, an inhibitor of tankyrase 1 and 2 which stabilizes axis inhibition protein (Axin), thereby reinforcing the β-catenin destruction complex. As ICG-001 proved most effective in attenuating ASM growth and ECM remodelling, we further explored the effects of this compound *in vivo* by investigating its ability to prevent ASM remodelling in a chronic mouse model of allergic asthma.

Methods

Cell culture

Three human bronchial smooth muscle cell lines, immortalized by stable expression of human telomerase reverse transcriptase (hTERT), were used for all experiments. The generation of these cell lines has been described previously (Gosens *et al.*, 2006). Cells were used up to passage 30 for all experiments. Cells were grown in uncoated 100/20 mm tissue culture dishes (GBO, #664160) in DMEM (GIBCO, #42430-082) supplemented with 200 U mL^{-1} penicillin–streptomycin (GIBCO, #15070-063), 2.5 μg mL^{-1} antimycotic (GIBCO, #15290-026) and 10% v v^{-1} FBS (Thermo Scientific, #SV30180.03).

TOPFLash assay

Cells grown in DMEM supplemented with antibiotics, antimycotics and 10% v v^{-1} FBS were seeded on uncoated 6-wells plates (Sigma Aldrich, #CLS3506) (300.000 cells per well) and were serum-starved after attachment for 12 h in plain DMEM. Cells were transfected for 24 h with either 1 μg TOPFlash (Addgene, #12456) or FOPFlash (Addgene, #12457) reporter plasmids using the TransIT-X2 transfection delivery system (Mirus, #MIR6000). Following transfection, cells were washed with PBS and subjected to stimulation. Luciferase activity was assayed with the Dual-Luciferase Reporter assay system (Promega, #E1910) according to the manufacturer's instructions.

Western blot analysis

Cells were washed with PBS and incubated with RIPA lysis buffer (65 mM Tris, 155 mM NaCl, 1% Igepal CA-630, 0.25% sodium deoxycholate, 1 mM EDTA, pH 7.4 and a mixture of protease inhibitors: 1 mM Na_3VO_4, 1 mM NaF, 10 μg mL^{-1} leupetin, 10 μg mL^{-1} pepstatin A, 10 μg mL^{-1} aprotinin). Cells were then scraped from the plate and kept on ice for 15 min. Lysates were vortexed vigorously and finally centrifuged for 10 min at 10 000 *g*. Lung homogenates were first pulverized with a pestle and mortar in liquid nitrogen and subsequently sonicated in RIPA. Following sonication, samples were processed in the same way as the cell lysates. Protein content of the supernatant fractions was determined with a BCA protein assay kit (Thermo Scientific, #23 225) and subsequently subjected to SDS-PAGE, using 6 and 10% running gels (depending on protein size). Separated proteins were transferred to either nitrocellulose (Bio-rad, 0.2 μm, #162-0112) or PVDF membranes (Carl Roth, 0.45 μm, #T830.1), which were then blocked with ROTI®-Block blocking solution (Carl Roth, #A151.2) for 2 h at room temperature. Membranes were incubated with primary antibodies overnight at 4°C in Tris-buffered saline-tween (TBST; 50 mM Tris–HCl, 150 mM NaCl, 0.05% w v^{-1} Tween-20, pH 7.4). The next day, after being washed in TBST, membranes were incubated with HRP-conjugated secondary antibody for 2 h at room temperature. Finally, blots were developed using enhanced chemiluminescence substrate (Perkin Elmer, #NEL105001EA). Digital images were quantified by densitometry using LI-COR Image Studio Lite software.

Cell proliferation assay

Cellular viability, or the reductive potential of the cell population, was measured with an Alamar Blue conversion assay, the conversion of which is proportional to cell number (Invitrogen, #DAL1100). Cells grown in DMEM supplemented with antibiotics, antimycotics and 10% v v^{-1} FBS were seeded on uncoated 24-well plates (Sigma Aldrich, #CLS3524) (30.000 cells per well) and were serum-starved after attachment for 3 days in serum-free DMEM supplemented with 1% insulin, transferrin and selenium (GIBCO, #51 300). Following stimulation for 48 h, cells were washed with PBS and incubated with 10% alamarBlue® reagent together with 1× HBSS (GIBCO, #14 065) at 37°C for 30 min. The supernatant was collected and fluorescence was measured in a 96-well plate (Sigma-Aldrich, #CLS3596) with excitation wavelength at 530 nm and emission wavelength at 590 nm.

RT-qPCR

Cells were washed with PBS and incubated with lysis buffer before being scraped from the plate. Lung homogenates were first pulverized with a pestle and mortar in liquid nitrogen prior to addition of lysis buffer. Isolation of mRNA was performed with a NucleoSpin® RNA isolation kit (Macherey-Nagel, # 740955.250) according to the manufacturer's instructions. Equal amounts of cDNA were synthesized using AMV reverse transcriptase (Promega, #A3500) and diluted 15 times with RNAse-free ddH_2O. Quantitative real-time PCR was performed on an Illumina Eco real-time PCR system using SYBR green as the DNA binding dye (Roche, #04913914001). PCR cycling was performed with denaturation at 94°C for 30 s, annealing at 60°C for 30 s and extension at 72°C for 30 s for 45 cycles. Analysis of RT-qPCR data was done using LinRegPCR analysis software (Ruijter *et al.*, 2009, 2013). 18S ribosomal RNA, β-2-microglobulin and ribosomal protein L13A were used as reference loci for accurate normalization of the RT-qPCR data. Primer sequences are listed in Table 1. Total RNA yield was determined with a NanoDrop ND-1000 spectrophotometer, and samples were normalized accordingly.

Animals

All procedures described in this study were approved by the animal ethics committee (DEC) of the University of Groningen under license number DEC-6485. Animal studies are reported in compliance with the ARRIVE guidelines (Kilkenny *et al.*, 2010; McGrath & Lilley, 2015). Inbred female

Table 1

Primer sequences used

Amplicon	Species	Forward sequence (5'→3')	Reverse sequence (5'→3')
Collagen 1α1	Homo sapiens	TCAGCAAGAACCCCAAGGAC	CCGCCATACTCGAACTGGAAT
18S ribosomal RNA	Homo sapiens	CGCCGCTAGAGGTGAAATTC	TTGGCAAATGCTTTCGCTC
B2M	Homo sapiens	AAGCAGCATCATGGAGGTTTG	AAGCAAGCAAGCAGAATTTGGA
RPL13A	Homo sapiens	ACCGCCCTACGACAAGAAAA	GCTGTCACTGCCTGGTACTT
WISP 1	Mus musculus	CAATAGGAGTGTGTGCACAGGT	CTCGCCATTGGTGTAGCGTA
Axin 2	Mus musculus	TCCTTACCGCATGGGGAGTA	CGGTGGGTTCTCGGAAAATG
cMyc	Mus musculus	CGACTCTGAAGAAGAGCAAGAAGA	GTAGTTGTGCTGGTGAGTGGA
18S ribosomal RNA	Mus musculus	AAACGGCTACCACATCCAAG	CCTCCAATGGATCCTCGTTA
B2M	Mus musculus	ACCGTCTACTGGGATCGAGA	TGCTATTTCTTTCTGCGTGCA
RPL13A	Mus musculus	AGAAGCAGATCTTGAGGTTACGG	GTTCACACCAGGAGTCCGTT

BALB/c mice (n = 10 per group) were obtained from Charles River (Leiden, The Netherlands). Animals were group-housed (10 per cage) in climate-controlled animal quarters and provided with food and water *ad libitum*. A 12 h/12 h light/dark cycle was maintained. Animals were 8–12 weeks of age at the start of the experiment, weighed 16–20 g and were randomly assigned to the different experimental groups. Group sizes were calculated based on airway eosinophil infiltration. Earlier studies with the ovalbumin (OVA)-challenge model within the University Medical Centre Groningen have shown an average of 16 ± 5 eosinophils (Melgert *et al.*, 2007). Assuming equal variance, α of 0.05, 1-β of 0.8 and an effect size of 40%, a group size of 10 can be obtained. Some samples were lost either due to death of the animals or post-processing issues of the animal tissue. These samples were not replaced as the OVA-challenge for this particular group of animals yielded a very robust infiltration of airway eosinophils (average of 30 ± 3 for the OVA-treated animals), almost twice the size of earlier studies and therefore maintaining sufficient power.

Allergen exposure

To induce a chronic allergic asthmatic response, animals were sensitized to chicken-derived OVA (Sigma-Aldrich, #A5378), using aluminum hydroxide ($AlOH_3$) (Imject™, Thermo Scientific, #77161) as an adjuvant to promote an IgE and Th2 skewed response, as previously described (Temelkovski *et al.*, 1998) (Figure 1). In brief, animals were sensitized on days 1, 14 and 21 by means of an i.p. injection of 10 µg OVA together with 1.5 mg of $AlOH_3$ dissolved in 200 µL saline. Subsequently, animals were exposed to aerosolized OVA (1% w v^{-1} in saline) or saline for 20 min day^{-1} on two consecutive days each week for 4 weeks. Exposures were carried out in a custom-built Perspex chamber (9 L) with a De Vilbiss Model 646 nebulizer. Air flow was set at a rate of 40 L min^{-1}, providing aerosol with an output of 0.33 mL min^{-1}. Thirty minutes prior to each challenge, 30 µL PBS containing ICG-001 (0.1, 0.33 and 1.0 mM) or DMSO as a vehicle control, was briefly vortexed and administered endotracheally via intranasal instillation immediately after brief exposure (circa 10 s) to 5% isoflurane.

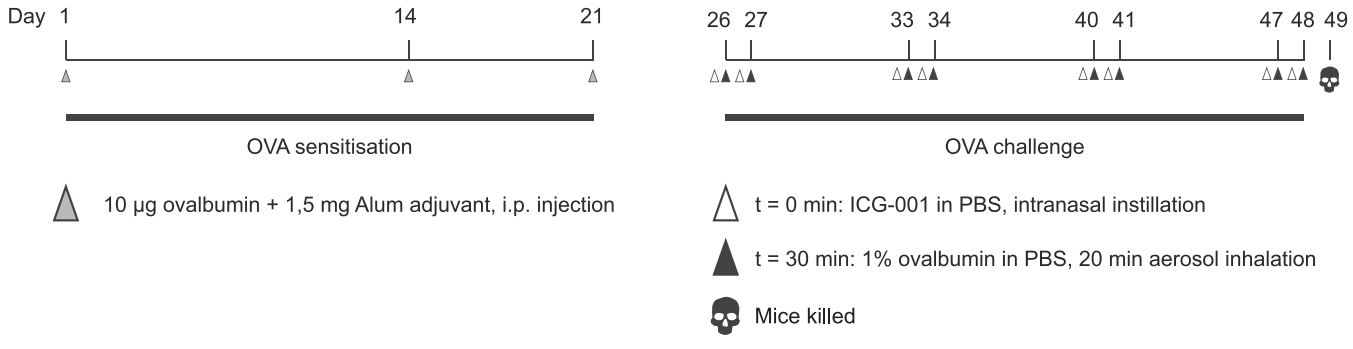

Figure 1

Experimental procedure for the chronic allergic (OVA) asthma mouse model. Mice were initially sensitized to OVA on days 1, 14 and 21 and subsequently challenged with saline or OVA aerosols for four consecutive weeks. ICG-001 or DMSO as a vehicle control was delivered intranasally via instillation 30 min prior to each challenge.

Blood and tissue collection

Twenty-four hours following cessation of the last inhalational exposure, animals were killed by exsanguination following a s.c. injection of 40 mg kg^{-1} ketamine and 0.5 mg kg^{-1} dexmedetomidine dissolved in 100 μL solvent. Then 0.5–1.0 mL blood was collected via cardiac puncture in 1.5 mL Eppendorf tubes and spun down to obtain serum. Lungs were harvested as follows: the post-caval, inferior lobe and left lobe were snap frozen in liquid nitrogen for mRNA and protein analysis. The leftover lungs were then inflated with 600 μL of a saline/Tissue-Tek® mixture (1:1 v v^{-1}), of which the superior lobe was subsequently fixed in formalin and later embedded in paraffin for immunohistochemistry. The middle lobe was snap frozen in liquid nitrogen and used for immunohistochemistry.

Immunofluorescence

Tissue-Tek®-perfused mouse lung tissue was cut with a Microm HM 525 (Thermo Scientific). Transverse cross sections of 5 μm were used for analyses. In short, sections were washed in PBS and fixed in ice-cold acetone for 15 min at 4°C. The sections were then incubated with PBS containing 0.3% Triton X-100 for 5 min and then blocked in 10% normal goat serum with 1% BSA in PBS. After being blocked, cells were incubated with primary antibodies diluted with 1% BSA in PBS overnight at 4°C, washed with PBS and incubated with fluorescent secondary antibody for 1 h at room temperature. Finally, sections were incubated with Hoechst 33342 nucleic acid stain (Invitrogen, #H1399), washed in ddH_2O and mounted with ProLong® Gold antifade (Molecular Probes, #P36930).

Mean fluorescence intensity was digitally analysed with ImageJ (NIH) software. Following a 300px background subtraction, images were thresholded, and the integrated density per area from the appropriate channel was calculated, using the perimeter of the ASM relative to Hoechst 33342 nucleic acid stain. Sections were observed through an HC PL APO CS2 63×/1.4 (oil) objective on a Leica SP8 Confocal Microscope (DMI 600). Analyses were performed in a blinded fashion. This experiment was performed at the UMCG Microscopy and Imaging Centre, which is sponsored by NWO-grants 40-00506-98-9021 (*TissueFaxs*) and 175-010-2009-023 (*Zeiss 2p*), University of Groningen.

Patient material

β-catenin staining was performed on de-identified asthmatic and non-asthmatic donor lungs not suitable for transplantation and donated for medical research, which were obtained through the International Institute for the Advancement of Medicine (Edison, NJ). Subject characteristics were as listed previously (Hackett *et al.*, 2013). The study was approved by the ethics committees of the institutions involved.

Immunohistochemistry

Paraffin-embedded lung tissue was cut with a Microm HM 340E microtome (Thermo Scientific). Transverse cross sections of 5 μm were used for analyses. In short, tissue sections were deparaffinised in xylene and rehydrated in a serial dilution of ethanol. Heat-induced epitope retrieval was performed where necessary in a Decloaking chamber™ Nxgen pressure cooker (Biocare Medical). Sections were washed in PBS and blocked in normal serum from the species in which the secondary antibody was generated [either goat (Dako, #X0907) or rabbit (Dako, #X0902)]. Primary antibody diluted in 1% BSA in PBS was incubated overnight at 4°C, then washed with PBS and incubated with 0.3% H_2O_2 in PBS for 15 min. Subsequently, sections were incubated with secondary antibody for 1 h at room temperature. Finally, sections were washed with PBS and developed with diamonibenzidine (Sigma-Aldrich, #D5637) for 5 min, followed by a haematoxylin counterstain (Sigma-Aldrich, #MHS32). Sections were then rinsed in tap water for 5 min, dehydrated in ethanol-xylene and mounted with KP-mounting medium (Klinipath, #7275).

Total collagen concentrations were visualized with a Sirius red stain. In short, tissue sections were deparaffinised in xylene and rehydrated in a serial dilution of ethanol. Sections were incubated in Sirius red solution (Sirius red F33: Klinipath, #80115, picric acid: Sigma-Aldrich, #P6744) for 60 min at room temperature, followed by a 2 min wash with 0.01 N HCl. Sections were counterstained with haematoxylin (Sigma-Aldrich, #MHS32) for 5 min, rinsed with tap water for 5 min, quickly dehydrated in ethanol-xylene and mounted with KP-mounting medium (Klinipath, #7275).

Mucous was visualized with a periodic acid Schiff (PAS) stain. Tissue sections were deparaffinised and hydrated to deionized water. Sections were immersed in periodic acid solution (Sigma-Aldrich, #3951) for 15 min at room temperature, rinsed in water and immersed in Schiff's reagent (Sigma Aldrich, #3952016) in the dark for 30 min at room temperature. Sections were rinsed in water, counterstained with haematoxylin (Sigma-Aldrich, #MHS32) for 5 min, rinsed with tap water for 5 min, quickly dehydrated in ethanol-xylene and mounted with KP-mounting medium (Klinipath, #7275).

Digital images were quantified using ImageJ (NIH). Analyses were performed in a blinded fashion. Expression intensity was expressed as staining positive area relative to the length of the basement membrane squared (mm^2 mm^{-2}).

Statistical analysis

All *in vitro* data represent the mean ± SEM, of at least four independent experiments, whereas for the *in vivo* experiments, at least seven animals were analysed per treatment group. In line with BJP guidelines, data with an n below five were not statistically analysed. A Shapiro–Wilk's test ($P > 0.05$) as well as visual inspection of the respective histograms, normal Q-Q plots and box plots were used to determine whether samples were normally distributed (approximately), using IBM SPSS Statistics version 23. Comparisons between two groups were made using Student's unpaired t-test for normally distributed data or a Mann–Whitney U-test as the non-parametric equivalent. Comparisons between three or more groups were performed using a one-way ANOVA followed by Tukey's *post hoc* test for normally distributed data, or with a Kruskal–Wallis H-test for non-normally distributed data. A value of $P < 0.05$ was considered statistically significant. Analyses were performed with GraphPad Prism (GraphPad Software, Inc.). The data and statistical analysis comply with the recommendations on experimental design and analysis in pharmacology (Curtis *et al.*, 2015).

Antibodies and chemicals

The following antibodies were used: GAPDH (western blot 1:3000, mouse, Santa Cruz, #sc-47724), phospho-Rb (western blot 1:500, rabbit, Cell Signaling, #9308), α-smooth muscle actin (α-SMA; immunohistochemistry 1:100, Abcam, #ab5694), collagen 1α1 (western blot 1:1000, goat, SouthernBiotech, #1310-01), β-catenin (western blot 1:1000, immunofluorescence 1:300, mouse, BD Biosciences, #610154), non-phospho (active) β-catenin (western blot 1:500, immunofluorescence 1:300, rabbit, Cell Signaling, #8814), peroxidase-conjugated anti-mouse IgG (western blot 1:3000, rabbit, Sigma-Aldrich, #A9044), peroxidase-conjugated anti-rabbit IgG (western blot 1:3000, goat, Sigma-Aldrich, #A0545), peroxidase-conjugated anti-goat IgG (western blot 1:8000, rabbit, Sigma-Aldrich, #A5420) and Alexa Fluor® 633-conjugated anti-rabbit IgG (immunofluorescence 1:500, goat, Invitrogen, #A-21070).

Other reagents used include the following: DMSO (Sigma Aldrich, #472301), (6S,9aS)-Hexahydro-6-[(4-hydroxyphenyl) methyl]-8-(1-naphthalenylmethyl)-4,7-dioxo-N-(phenylmethyl)-2H-pyrazino[1,2-a]pyrimidine-1(6H)-carboxamide (ICG-001) (Tocris, #4505), 3,5,7,8-Tetrahydro-2-[4-(trifluoromethyl)phenyl]-4H-thiopyrano[4,3-d]pyrimidin-4-one (XAV-939) (Tocris, #3748), 2-[2-(4-Acetylphenyl)diazenyl]-2-(3,4-dihydro-3,3-dimethyl-1(2H)-isoquinolinylidene)acetamide (IQ-1) (Tocris, #4713), recombinant TGFβ1 (R&D Systems, #240-B), recombinant PDGF (Sigma-Aldrich, #P332G), ProLong® Gold Antifade Mountant (Molecular Probes, #P36930), Hoechst 33342 (Molecular Probes, #H3570) and FBS (Thermo Scientific, #SV30180.03). All other chemicals were of analytical grade.

Results

Small-molecule compounds effectively inhibit β-catenin function in ASM cells

Three commercially available compounds were selected for this study: ICG-001 [inhibits β-catenin/CBP interaction, IC_{50} 3 μM (Eguchi *et al.*, 2005)], IQ-1 [prevents β-catenin/p300 interaction, IC_{50} 2 μM (Miyabayashi *et al.*, 2007)] and XAV-939 [a WNT-specific β-catenin antagonist that inhibits tankyrase 1 and 2 to stabilize Axin, IC_{50} 4/11 nM respectively (Huang *et al.*, 2009)]. A TOPFlash reporter assay was used to establish their effects on β-catenin-mediated T-cell factor (TCF)-dependent gene transcription. TOPflash constructs contain copies of wild-type TCF/LEF binding sites upstream of a luciferase reporter, whereas the FOPflash contains mutated TCF/LEF binding sites. All three compounds were able to attenuate FBS-induced β-catenin/TCF target gene transcription (Figure 2A) in cultured ASM cell lines. As XAV-939 affects global levels of active β-catenin, the TOPFlash results were corroborated with a Western Blot. As expected, treatment with XAV-939 inhibited protein levels of non-phospho (active) β-catenin, whereas levels of total β-catenin remained unaffected (Figure 2B). In line with this, ICG-001 and IQ-1 did not affect β-catenin expression (Figure 2C).

Inhibition of β-catenin/CBP reduces ASM cell proliferation in vitro

ASM actively utilizes β-catenin to induce cell proliferation (Nunes *et al.*, 2008; Gosens *et al.*, 2010). To further investigate

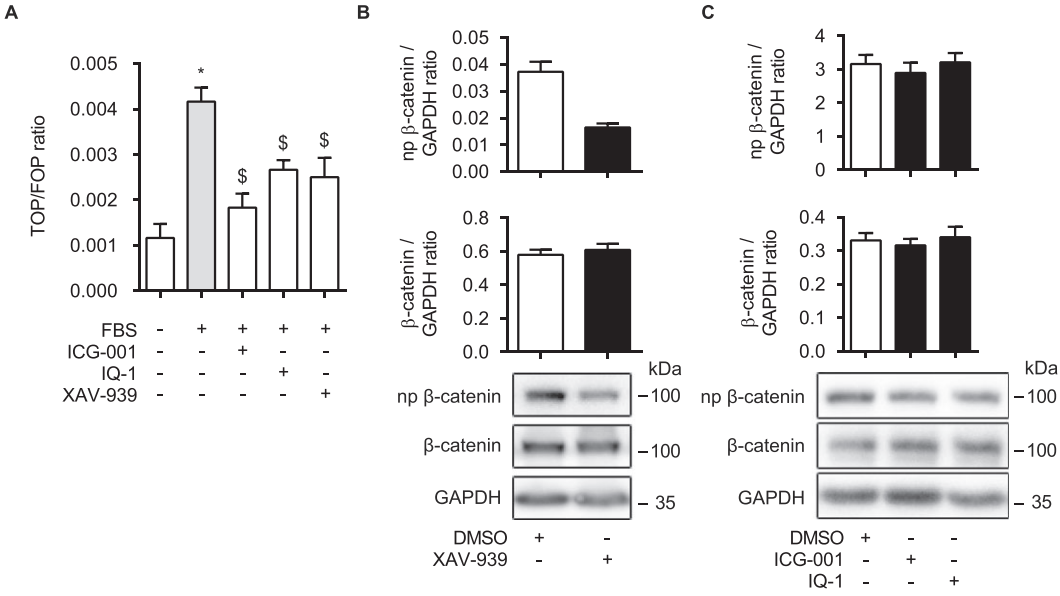

Figure 2

Small-molecule compounds inhibit β-catenin *in vitro*. (A) TOPFlash reporter assay of immortalized human airway smooth muscle (ASM) cells exposed to 10% FBS for 24 h with or without ICG-001, IQ-1 or XAV-939 (3 μM). Data represent six independent experiments. (B) and (C) Non-phosphorylated and total β-catenin immunoblot of lysates from cultured human ASM cells, normalized against GAPDH. Cells were treated with XAV-939, ICG-001 or IQ-1 (10 μM) for 16 h. Data represent four independent experiments. Data are expressed as the mean ± SEM. * Significant versus control, $ versus FBS.

this relationship and the specific mechanisms involved, we studied the effects of small-molecule inhibition. Cells were treated with FBS in combination with increasing concentrations of ICG-001, IQ-1 or XAV-939. After which, the reductive capacity of the cells as an indicator for cell number was measured with an Alamar Blue conversion assay. ICG-001 and XAV-939 dose-dependently inhibited FBS-induced Alamar Blue fluorescence intensity (63 and 48% reduction respectively), whereas IQ-1 had no effect (Figure 3A). To confirm whether these results were due to cellular proliferation, protein levels of phosphorylated Rb (pRB) were assessed as a marker for cell-cycle progression. ICG-001 inhibited FBS-induced expression of pRB by 68% at 3 μM compared with DMSO-treated cells (Figure 3B). IQ-1 and XAV-939 both appeared to decrease pRb expression, albeit non-significantly, and were markedly less effective at this than ICG-001 (Figure 3B). To further elaborate on the underlying mechanisms involved, we followed up on these experiments by using the receptor tyrosine kinase (RTK) agonist PDGF, which drives nuclear β-catenin accumulation through Akt and GSK-3β. Similar to the FBS-induced results, ICG-001 but also IQ-1 strongly inhibited PDGF-induced phosphorylation of Rb (78 and 62% reduction at 3 μM for ICG-001 and IQ-1 respectively) (Figure 3C). Again, XAV-939 was less effective, failing to induce a statistically significant reduction (Figure 3 C). Together, the data show that inhibition of β-catenin signalling via CBP or p300 effectively attenuates ASM proliferation.

Impaired collagen 1α1 production following β-catenin inhibition in vitro

Whereas TGFβ1 has weak mitogenic effects in ASM cells (Oenema *et al.*, 2013), it is a potent regulator of the expression of various ECM genes in ASM, which underlies both inhibition of GSK-3β as well as *de novo* synthesis of β-catenin (Baarsma *et al.*, 2011). To further explore this principle, we investigated the effects of β-catenin inhibition on ECM production by ASM cells, exposing cells to TGFβ1 co-treated with either ICG-001, IQ-1 or XAV-939. Both mRNA and protein

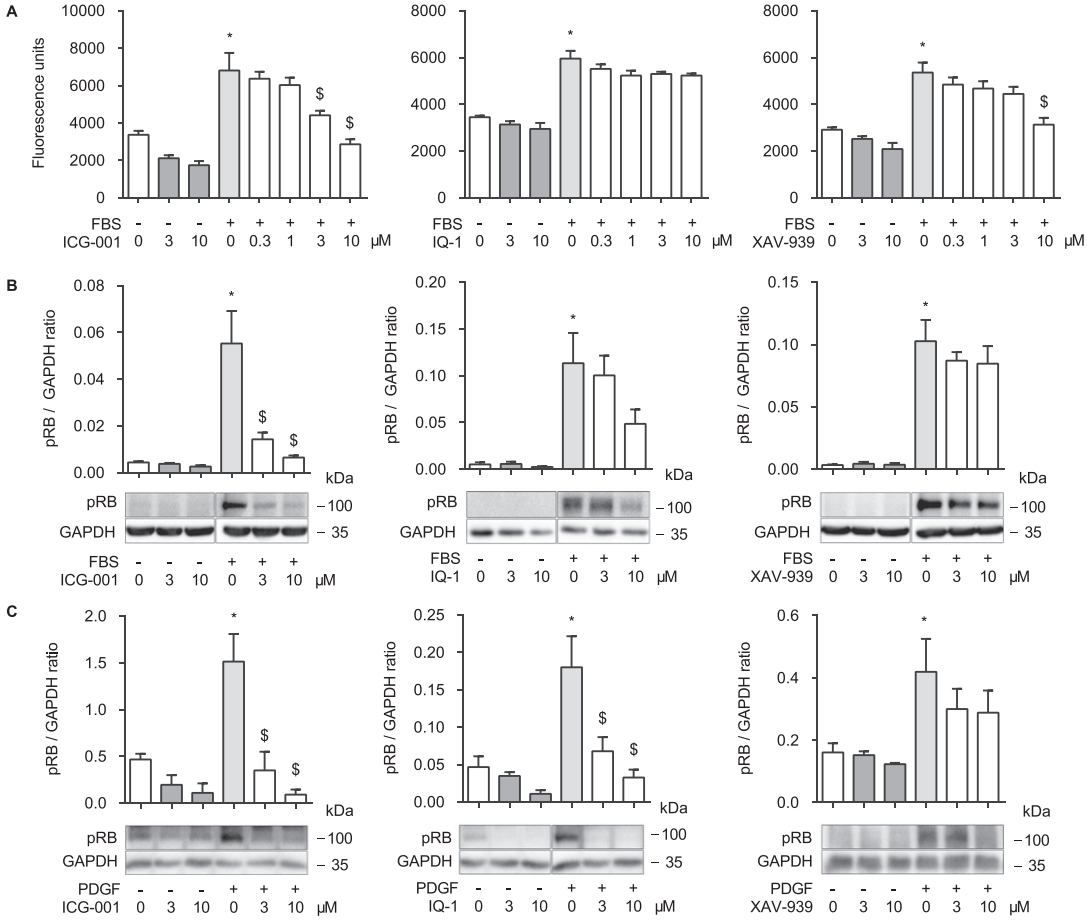

Figure 3

β-catenin inhibition reduces the proliferation of airway smooth muscle (ASM) cells *in vitro*. (A) Alamar Blue viability assay of immortalized human ASM cells exposed to 10% FBS for 48 h with or without ICG-001, IQ-1 or XAV-939 (0.3–10 μM). Data represent six independent experiments. (B) and (C) Phosphorylated (Ser $^{807/811}$) Rb (pRB) immunoblot indicative of G1 cell-cycle progression, normalized against GAPDH. Cells were treated with either 10% FBS or 50 ng mL^{-1} PDGF with or without ICG-001, IQ-1 or XAV-939 (3 and 10 μM) for 16 h. Data represent five, seven and five independent experiments for ICG-001, IQ-1 and XAV-939 treated samples respectively for (B) and five independent experiments for (C). Data are expressed as the mean ± SEM. * Significant versus control, $ versus FBS or PDGF.

levels were measured. Cells treated with ICG-001 exhibited a significant dose-dependent reduction in TGFβ1-induced gene expression of collagen 1α1 (47% reduction at 3 μM) (Figure 4 A, left upper panel). These findings were corroborated at the protein level (67% reduction at 3 μM) (Figure 4B, left panel). XAV-939 did not decrease mRNA abundance, but did reduce protein expression, although not to the same extent as ICG-001 (39% reduction at 3 μM) (Figure 4A–B, right panels). Interestingly, IQ-1 treatment resulted in an increase in TGFβ1-induced expression of collagen 1α1 mRNA, yet with a decreased protein expression (58% reduction at 3 μM) (Figure 4A–B, middle panels). In terms of mRNA expression, ICG-001 also proved most effective for the other TGFβ1 target genes connective TGF and fibronectin I (Figure 4A, middle and lower panels).

Expression of target genes, but not β-catenin itself is increased in OVA-challenged mice

ICG-001 demonstrated superior effects over IQ-1 and XAV-939 in terms of inhibition of ASM cell proliferation and ECM production. For that reason, we selected ICG-001 for subsequent *in vivo* studies to assess the effect of CBP/β-catenin inhibition on airway remodelling using a chronic OVA mouse model. OVA induces a robust pulmonary inflammatory response. The model is widely used to reproduce the pathophysiology of clinical (allergic) asthma and displays many features of airway remodelling similar to the disease (Nials and Uddin, 2008). Interestingly, repeated OVA challenge did not induce differences in either total or non-phosphorylated (active) β-catenin levels in the ASM bundle of frozen lung tissue sections (Figure 5A–B). The fluorescence

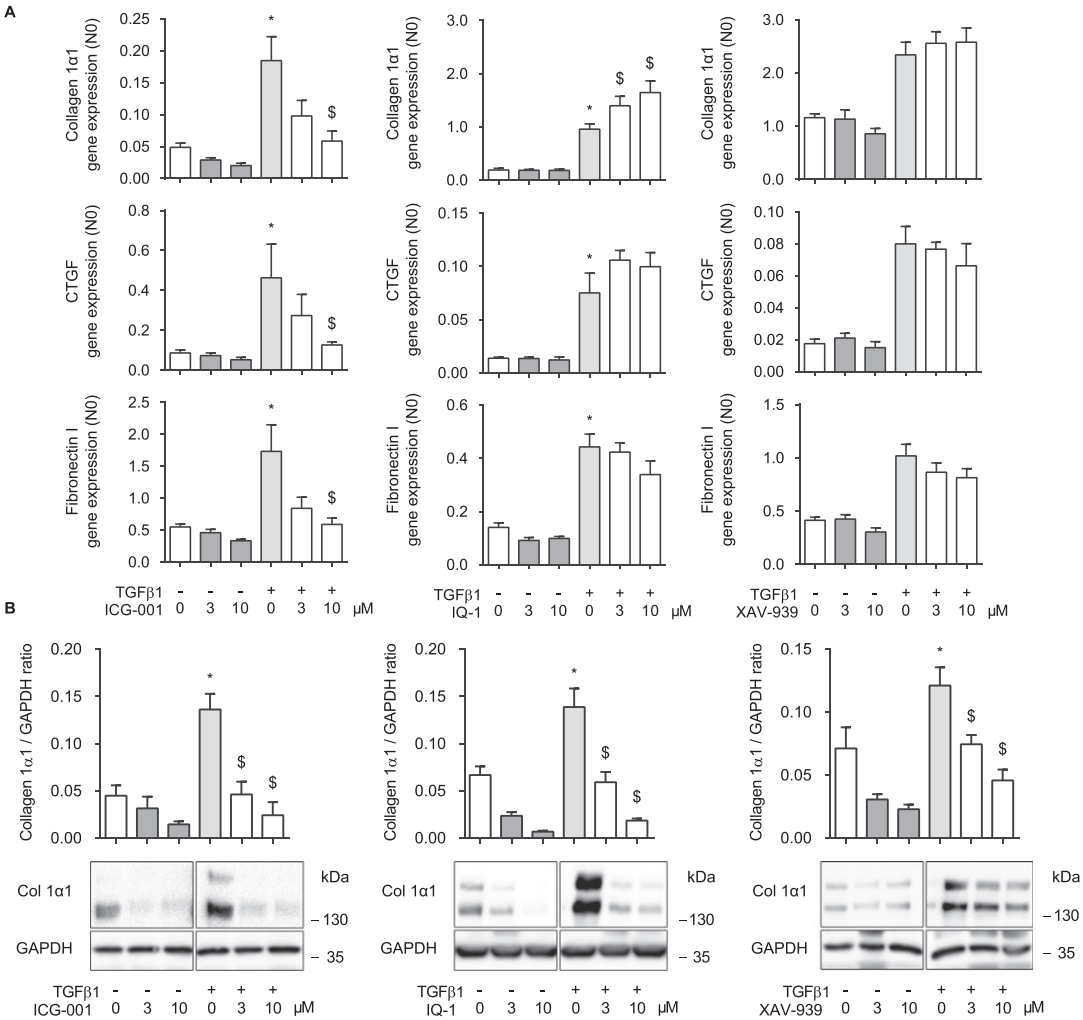

Figure 4

Impaired collagen 1α1 production following β-catenin inhibition *in vitro*. (A) mRNA of airway smooth muscle (ASM) cells pre-incubated with TGFβ1 (2 ng mL^{-1}) for 24 h with or without ICG-001, IQ-1 or XAV-939 (3 and 10 μM) was isolated and subjected to RT-qPCR. Bars represent collagen 1α1 gene expression. Data represent five, eight and four independent experiments for ICG-001, IQ-1 and XAV-939 treated samples respectively. (B) Collagen 1α1 immunoblot, normalized against GAPDH. Cells were treated with TGFβ1 (2 ng mL^{-1}) for 48 h with or without ICG-001, IQ-1 or XAV-939 (3 and 10 μM). Data represent five independent experiments. Data are expressed as the mean ± SEM. * Significant versus control, $ versus TGFβ1.

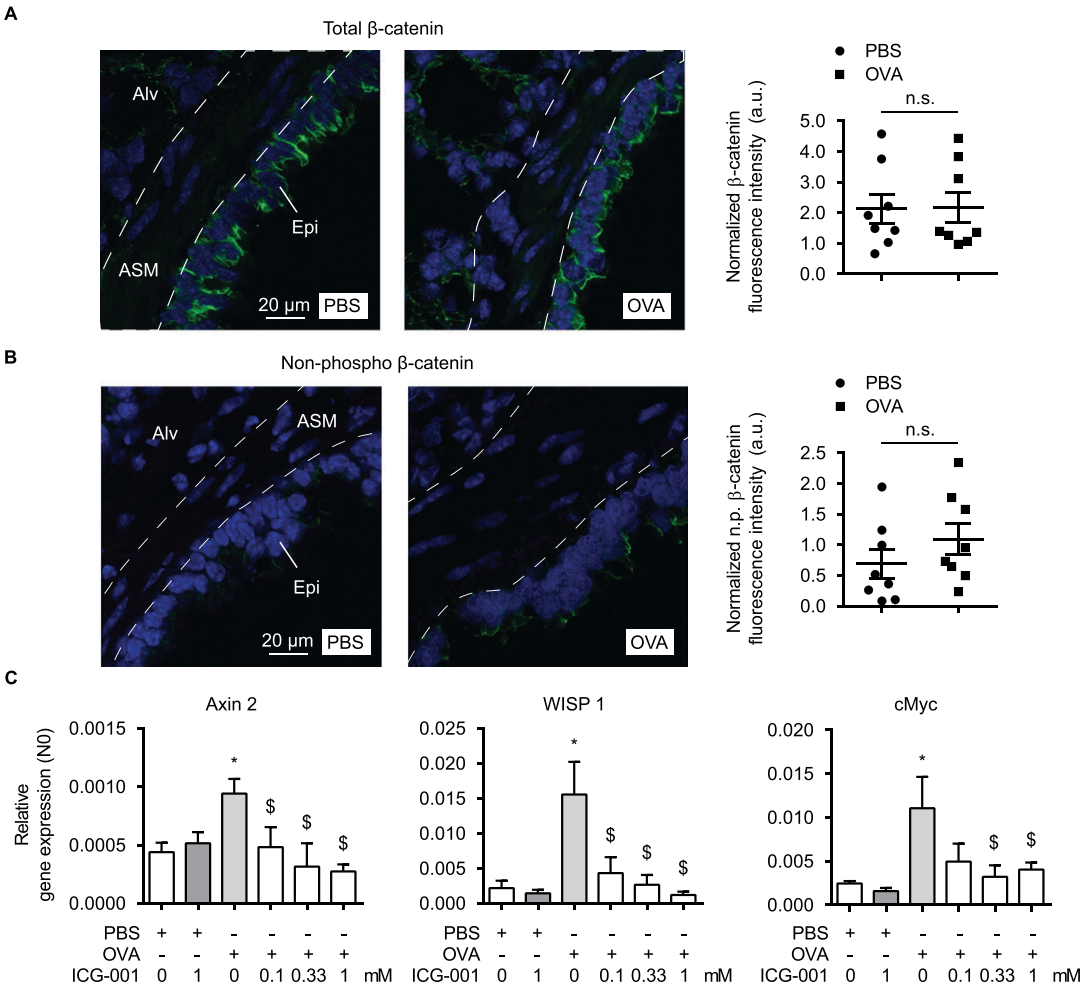

Figure 5

β-catenin (target gene) expression in OVA-challenged mice. (A) Representative immunofluorescent image (left) and the quantification (right) of total β-catenin (green colour), normalized to DAPI from frozen lung tissue sections of mouse airways exposed to repeated allergen (OVA) challenge versus PBS-treated controls. Nuclear DAPI staining is represented by blue. Dashed line represents the ASM boundary. Alv is alveoli, Epi is epithelium. Each dot represents a single animal. (B) Immunofluorescent image of non-phosphorylated (active) β-catenin as in (A). (C) mRNA of whole lung homogenates subjected to RT-qPCR, obtained from animals exposed to OVA or PBS and treated with intranasally instilled ICG-001. Group sizes are n = 9, 9, 9, 10, 8 and 7 for the respective groups (left to right). Data are expressed as the mean ± SEM. *Significant versus PBS, $ versus OVA.

staining intensity in the ASM bundle was also low compared with surrounding tissues, such as the epithelium. However, the expression of mRNA for the WNT1 inducible signalling pathway protein (WISP) 1, Axin 2 and cMyc, three well-known β-catenin target genes, was increased in whole lung homogenates of OVA challenged mice (738, 214 and 458% increase respectively vs. PBS-challenged mice) (Figure 5C). Moreover, topical treatment of the airways with intranasally instilled ICG-001 30 min prior to each challenge dose-dependently attenuated the OVA-induced increase in WISP 1, cMyc and Axin 2 gene expression (93, 71 and 63% reduction respectively for the 1 mM group vs. OVA). These data demonstrate that β-catenin expression in ASM does not appear to be altered under conditions of allergic airway inflammation, whereas its target genes WISP 1, Axin 2 and cMyc are differentially expressed in whole lung tissue, indicating activation of β-catenin-dependent gene transcription.

β-catenin expression does not change in ASM of mild to moderate asthmatics

The results obtained from the mouse model suggest that allergic airway inflammation does not change either the expression or the activation state of β-catenin in ASM. We wanted to know whether human asthmatic ASM would display a similar pattern. To evaluate the significance of targeting β-catenin-mediated transcription in asthma, we assessed the expression levels of total and non-phosphorylated β-catenin in the ASM bundle of tissue derived from mild to moderate asthmatic and non-asthmatic donor lungs. Similar to our

animal model, fluorescence emission of total β-catenin levels were no different in asthmatic ASM compared with non-asthmatic ASM (Figure 6A). We also performed immunohistochemistry, which revealed that the active form of β-catenin was also not differentially expressed between asthmatics and non-asthmatics (Figure 6B).

ICG-001 prevents OVA-induced airway smooth muscle remodelling

Because β-catenin-dependent gene transcription was elevated in our animal model, we assessed the ability of ICG-001 to reduce ASM bundle thickness and ECM production, using α-SMA and total collagen as a readout. Repeated OVA challenge increased α-SMA expression measured around the airways compared with the saline-treated group (158% increase vs. PBS-challenged mice). Interestingly, ICG-001 treatment fully reversed this process back to PBS-treated levels (44% reduction for the 0.1 mM group) (Figure 7A). Curiously, the smallest dose produced the strongest response, whereas the highest dose yielded no statistically significant difference in smooth muscle thickness. A Picro Sirius Red stain indicative of the total collagen deposited around the airways revealed increased production in the OVA-treated group (161% increase vs. PBS-challenged mice). A declining trend towards reduced collagen levels following ICG-001 treatment can be appreciated from the data, albeit without statistical significance (Figure 7B). Together, the data indicate that in an allergic environment, ICG-001 negatively affects ASM remodelling.

Eosinophil infiltration and mucous production is not affected by ICG-001 treatment

In addition to its ability to contract, the ASM also has an important secretory function in the airways. We were interested in whether ICG-001 could affect inflammatory events within the proximity of the ASM bundle. As expected, repeated OVA challenge increased the amount of mucous covering the airway lumen (OVA vs. PBS), as determined with a periodic acid-Schiff (PAS) stain. However, treatment with ICG-001 did not significantly negate the increased mucus area (Figure 8A). To extend these findings, we investigated the number of eosinophils that infiltrated around the airways, visualized by 3,3′-diaminobenzidine. While the number of eosinophils was greatly increased in the OVA-treated group, there was no statistically significant difference between OVA and any of the ICG-001-treated groups (Figure 8B).

Discussion

In this study, we evaluated the potential ability of three small-molecule compounds, ICG-001, IQ-1 and XAV-939, to inhibit β-catenin function *in vitro*. We demonstrated that

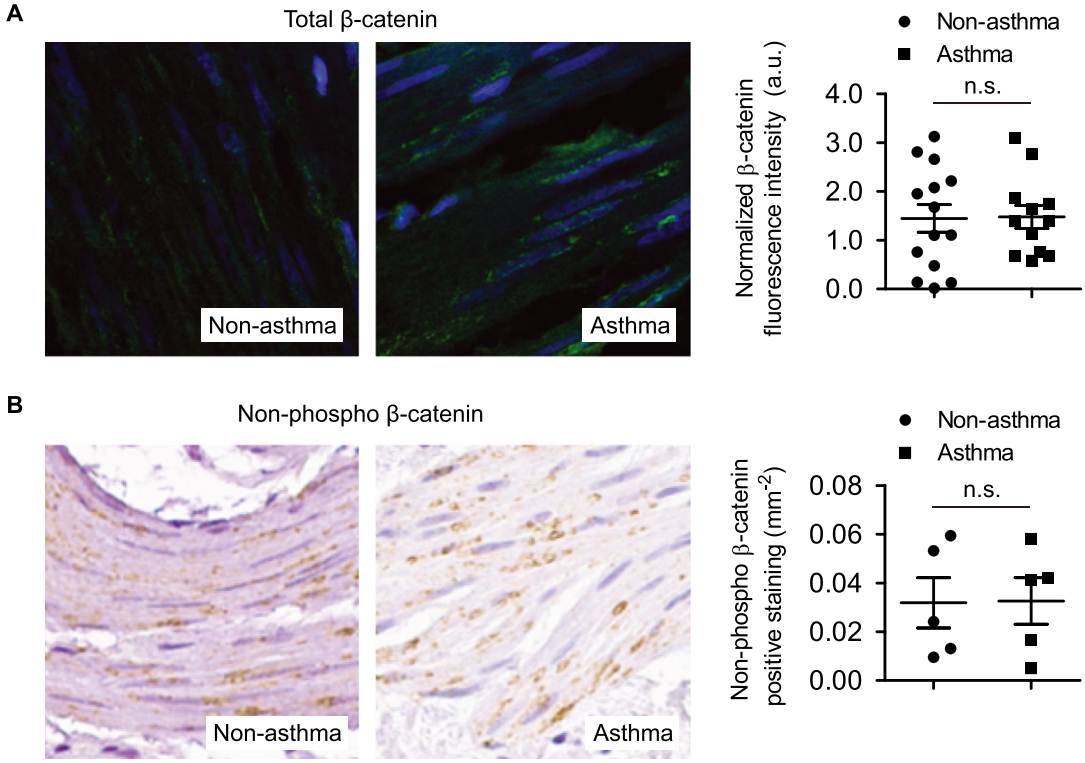

Figure 6

β-catenin expression in asthmatic airway smooth muscle (ASM). (A) Representative immunofluorescent image (left) and the quantification (right) of total β-catenin (green colour) from asthmatic and non-asthmatic donor ASM tissue, normalized to DAPI (blue colour). Two airways per donor were analysed. (B) Representative immunohistochemistry image (left) and the quantification (right) of non-phosphorylated (active) β-catenin (DAB) in asthmatic and non-asthmatic donor ASM tissue.

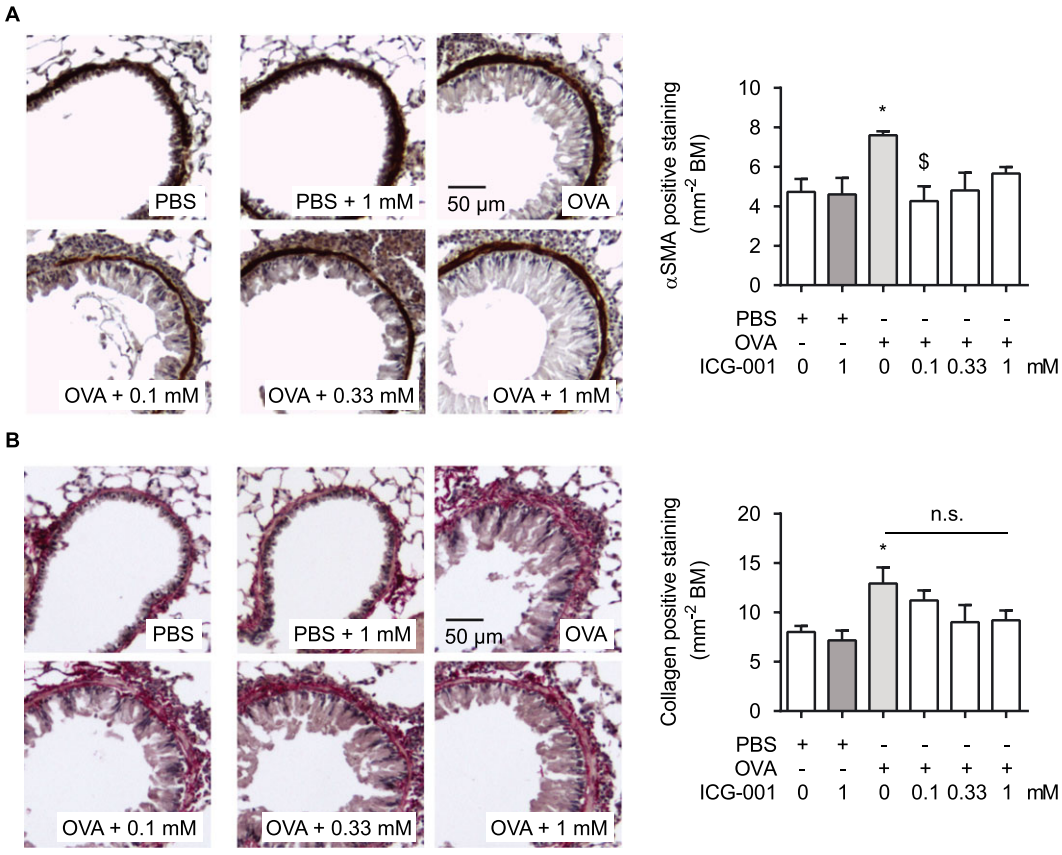

Figure 7

ICG-001 prevents OVA-induced airway smooth muscle (ASM) remodelling. (A) Representative immunohistochemistry images (left) and the quantification (right) of α-SMA staining visualized with DAB, obtained from paraffin-embedded lung tissue sections of mouse airways exposed to repeated allergen (OVA) challenge versus PBS-treated controls. Data represent at least seven animals. (B) Immunohistochemistry staining as in (A) of total collagen deposition, measured with a Sirius Red stain. Group sizes are n = 10, 10, 10, 8, 10 and 7 for the respective groups (left to right). Data are expressed as the mean ± SEM. *Significant versus PBS, $ versus OVA, basement membrane (BM).

treatment with ICG-001 effectively inhibits ASM cell cycle progression. The interaction of the co-activator CBP with β-catenin, rather than p300 or effectors that stabilize Axin, appears to be fundamental in the regulation of this process. These results fit the previously proposed model (Ma *et al.*, 2005) that the TCF/β-catenin/CBP interaction primarily initiates the gene transcription events associated with cellular proliferation, whereas the TCF/β-catenin/p300 interaction is more involved in driving normal cellular differentiation. In our study, there was some inhibition of cell growth following IQ-1 exposure, suggesting that in ASM cells, there may be some degree of redundancy between CBP/p300 function (Goodman and Smolik, 2000). Alternatively, differences in their endogenous expression levels could underlie the dissimilar response. IQ-1 exerts its action on p300 by inhibiting protein phosphatase 2A (PP2A). It does so by binding to its PR72 and PR130 subunits, resulting in decreased phosphorylation of p300 through an as yet undetermined mechanism. This reduces its binding affinity to β-catenin and thereby diminishing its interaction (Miyabayashi *et al.*, 2007). PR72 and PR130 expression levels have been reported to be very low in smooth muscle (Zwaenepoel *et al.*, 2008), possibly explaining the relative mild effects of IQ-1 on ASM proliferation. Interestingly, treatment with XAV-939 was unable to produce the same degree of inhibition as ICG-001, whereas the levels of non-phospho β-catenin were clearly diminished (Figure 2B). It is possible that only very low levels of β-catenin are required in the nucleus to induce cell growth and that the leftover pool after XAV-939 is sufficient for this effect. In addition, XAV-939 acts upon the β-catenin destruction complex and thus primarily influences WNT-dependent signalling. The results support the notion that FBS-induced proliferation in ASM may be more driven by WNT-independent mechanisms that stabilize β-catenin independently from the destruction complex.

We further showed that β-catenin is essential for the regulation of ECM production in ASM cells. CBP appears to be central in this event, as exposure to ICG-001 dose-dependently inhibited the synthesis of both collagen 1α1 mRNA and protein following TGFβ1 stimulation. Interestingly, exposure to IQ-1 dose-dependently increased the expression of mRNA for collagen 1α1, but decreased the protein yield. The discrepancy between mRNA and protein further demonstrates the complex interplay between CBP

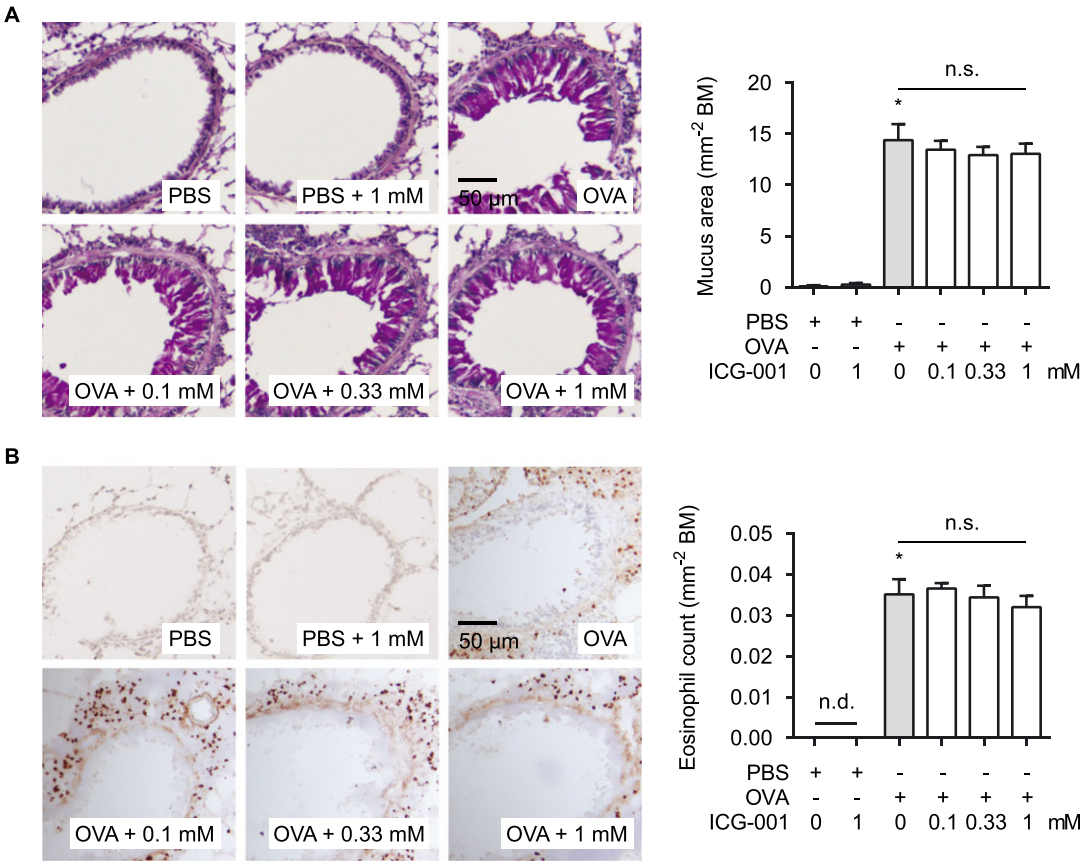

Figure 8

Effects of ICG-001 on eosinophil infiltration and mucous production**.** (A) Representative immunohistochemistry images (left) and the quantification (right) of a PAS stain, indicative of mucous, obtained from paraffin-embedded lung tissue sections of mouse airways exposed to repeated allergen (OVA) challenge versus PBS-treated controls. Data represent at least seven animals. (B) Immunohistochemistry staining as in (A) of eosinophil's endogenous peroxidase activity, measured with DAB. Group sizes are n = 10, 10, 10, 8, 10 and 7 for the respective groups (left to right). Data are expressed as the mean ± SEM. *Significant versus PBS, basement membrane (BM).

and p300 signalling or possibly off-target effects of IQ-1, and it was beyond the scope of this study to investigate the underlying principles further.

In our animal model, topical application of ICG-001 to the airways of BALB/c mice significantly reduced ASM mass induced by repeated allergen challenge. However, contrary to our *in vitro* findings, no changes in collagen content were found. This finding contradicts previous publications on β-catenin inhibition in murine models of fibrosis in the lung (Akhmetshina *et al.*, 2012; Ulsamer *et al.*, 2012), where pharmacological inhibition of β-catenin or overexpression of Dickkopf-1 ameliorates fibrosis. In one study, administration of ICG-001 in a bleomycin-mouse model prevented fibrosis, and its application at a later stage was able to reverse any established fibrosis (Henderson *et al.*, 2010). Various explanations may underlie these differences. An important distinction that has to be addressed here is the model used for experimentation. In the bleomycin model, fibrosis is initially induced by new collagen deposition, whereas the continued pathology results from the maintenance of th eestablished ECM and not due to newly synthesized collagen (Blaauboer *et al.*, 2013). In asthma, ECM turnover is significantly enhanced (Bousquet *et al.*, 1991; Meerschaert *et al.*, 1999), not only by the synthesis of new proteins and other components but also by its degradation through the activity of MMPs and tissue inhibitors of metalloproteinase (TIMPs; Johnson, 2005). Increased ECM turnover in the OVA model may have obscured any potential effects mediated by ICG-001. Alternatively, the overlapping functions of CBP and p300 may have contributed to the observed effect, as CBP and p300 may act redundantly in some cell systems. ICG-001 competes with β-catenin for CBP, resulting in increased binding of β-catenin to additional partners like p300 (Emami *et al.*, 2004). In this case, the application of ICG-001 would not be sufficient to achieve full inhibition. Moreover, in addition to the ASM, other cell types like myofibroblasts also contribute to peribronchial collagen deposition (Brewster *et al.*, 1990), and it is unclear at this moment what the relative contribution of each source is. In the light of this, TGFβ1-driven expression of collagen type 1 has been shown to be mediated via p300 in human fibroblasts (Ghosh *et al.*, 2000, 2001).

Little work has been done on WNT/β-catenin or TGFβ1/β-catenin signalling in the context of asthma. The growth of

smooth muscle in the developing mouse lung requires β-catenin signalling and its activity is increased following exposure to the allergen *Aspergillus fumigatus* (Cohen *et al.*, 2009). Furthermore, in primary bronchial epithelial cells, TGFβ1-induced epithelial to mesenchymal transition is paralleled by activation of β-catenin signalling, which is even further enhanced when the cells are exposed to house dust mite extract (Heijink *et al.*, 2010). In our study, we did not find any difference in either total or non-phosphorylated (active) β-catenin expression between healthy and asthmatic ASM lung tissue, and this finding was corroborated in our OVA mouse model. However, the expression of the β-catenin target genes WISP 1 and Axin 2 were increased in OVA challenged mice. Perhaps the limited proportion of total β-catenin translocating to the nucleus or differences between the time points at which translocation is observed (24 h after allergen challenge in our study) account for this apparent discrepancy. β-catenin is a pleiotropic gene, involved in many different cellular processes, and its activation needs to be tightly regulated to coordinate cell behaviour. This translates into transient periods of activation, where both activation and diminution act in quick succession. Exposure to allergens could initiate a cascade of events starting with activation of β-catenin and setting the stage for the development of airway remodelling. As such, it is possible that although activation of β-catenin is a critical initiating event in the pathogenesis of asthma, it eventually becomes superfluous in the face of additional downstream targets that accumulate over time. Additionally, even when there is no change in the total β-catenin pool, there may still be changes in protein binding mediated by β-catenin, driven by the presence of additional adapter proteins that may show altered expression in asthma. This results in enhanced β-catenin target gene transcription, without any change in β-catenin abundance itself. Finally, potential changes in β-catenin expression may be limited to only a few cells. Even within one individual, smooth muscle cells exhibit different phenotypes, some being synthetic and others being more contractile. As these phenotypes associate with different β-catenin expression levels (Nunes *et al.*, 2008), measuring the entire ASM pool will potentially mask changes in individual cells. To answer these questions, it is important that we gather more information about the temporal behaviour of β-catenin and to assess how β-catenin target genes behave in an asthmatic environment.

β-catenin signalling plays a crucial role in orchestrating developmental processes and maintaining tissue homeostasis in adult life. It is essential in virtually every organ system in homeostasis, including the lung. It is not surprising that its abnormal regulation is linked to such a vast array of diseases (Clevers and Nusse, 2012). Even within the lung, β-catenin signalling performs seemingly opposing roles in cellular proliferation and differentiation (Mucenski *et al.*, 2005). This is not unexpected, given the staggering amount of binding partners that β-catenin has, which modulate can a plethora of downstream biological processes. The ubiquitous nature of β-catenin signalling and its pleotropic effects make it problematic for specific targeting, particularly in a chronic setting, such as asthma. Successfully targeting β-catenin signalling in asthma requires careful balancing, as the inhibition of β-catenin in off-target tissues could cause unwanted effects. Now that we have begun to understand the crucial role of cofactors such as CBP and p300, and the disparate effects that they may mediate, new therapeutic avenues are beginning to emerge. ICG-001 holds much promise in this regard, as it disrupts only a very small subset of CBP interactions, initiating a transcriptional programme that inhibits ASM growth. At the same time, additional genes regulated by p300 or other cofactors that are important in maintaining cellular homeostasis are not affected by the therapy, something that would not be achieved by inhibiting β-catenin alone. This shows that inhibiting the interaction of β-catenin with CBP inhibition may be a successful strategy for preventing ASM thickening in a way that is independent of inflammation, which is of clear relevance to severe asthma, in which ASM remodelling persists despite treatment with corticosteroids.

In conclusion, we showed that the β-catenin/CBP interaction is essential for the regulation of ASM proliferation and production of ECM components. In our *in vivo* experiments, in spite of a lack of observable changes in β-catenin expression levels, the asthmatic airways exhibited enhanced β-catenin target gene transcription, which was inhibited by the administration of ICG-001. From this we concluded that inhibition of β-catenin results in diminished ASM thickness driven by repeated allergen challenge in a mouse model of allergic asthma, but has no effect on total collagen deposition. These findings highlight the importance of β-catenin/CBP signalling in the airways and suggest ICG-001 may be a new therapeutic approach to treat ASM remodelling in asthma.

Acknowledgements

This study was financially supported by an NWO Vidi grant (016.126.307). The authors wish to thank Sophie I Bos and Anita I Spanjer for helping with the collection of animal tissue as well as the preparation of the paraffin-embedded tissue.

Author contributions

T.K. conceived the study and designed the experiments, carried out the vast majority of the work, analysed the majority of the data and drafted the manuscript. S.C. carried out part of the *in vitro* work. M.M. carried out part of the *in vivo* work. T.L.H. and D.K. provided and conducted work on the patient material. A.J.H. kindly provided the human ASM cells. R.G. conceived the study and designed the experiments. All authors critically revised the manuscript for important intellectual content and approved its final version.

Conflict of interest

The authors declare no conflicts of interest.

Declaration of transparency and scientific rigour

This Declaration acknowledges that this paper adheres to the principles for transparent reporting and scientific rigour of

preclinical research recommended by funding agencies, publishers and other organisations engaged with supporting research.

References

Akhmetshina A, Palumbo K, Dees C, Bergmann C, Venalis P, Zerr P *et al.* (2012). Activation of canonical Wnt signalling is required for TGF-β-mediated fibrosis. Nat Commun 3: 735.

Alexander SPH, Kelly E, Marrion N, Peters JA, Benson HE, Faccenda E *et al.* (2015a). The Concise Guide to PHARMACOLOGY 2015/16: Overview. Br J Pharmacol 172: 5729–5143.

Alexander SPH, Fabbro D, Kelly E, Marrion N, Peters JA, Benson HE *et al.* (2015b). The Concise Guide to PHARMACOLOGY 2015/16: Enzymes. Br J Pharmacol 172: 6024–6109.

Baarsma H, Menzen M, Halayko A, Meurs H, Kerstjens H, Gosens R (2011). β-Catenin signaling is required for TGF-β1-induced extracellular matrix production by airway smooth muscle cells. Am J Physiol Lung Cell Mol Physiol 301: L956–L965.

Baarsma HA, Königshoff M, Gosens R (2013). The WNT signaling pathway from ligand secretion to gene transcription: molecular mechanisms and pharmacological targets. Pharmacol Ther 138: 66–83.

Barbato A, Turato G, Baraldo S, Bazzan E, Calabrese F, Panizzolo C *et al.* (2006). Epithelial damage and angiogenesis in the airways of children with asthma. Am J Respir Crit Care Med 174: 975–981.

Benayoun L, Druilhe A, Dombret M-C, Aubier M, Pretolani M (2003). Airway structural alterations selectively associated with severe asthma. Am J Respir Crit Care Med 167: 1360–1368.

Blaauboer ME, Emson CL, Verschuren L, van Erk M, Turner SM, Everts V *et al.* (2013). Novel combination of collagen dynamics analysis and transcriptional profiling reveals fibrosis-relevant genes and pathways. Matrix Biol J Int Soc Matrix Biol 32: 424–431.

Bousquet J, Chanez P, Lacoste JY, Enander I, Venge P, Peterson C *et al.* (1991). Indirect evidence of bronchial inflammation assessed by titration of inflammatory mediators in BAL fluid of patients with asthma. J Allergy Clin Immunol 88: 649–660.

Brewster CE, Howarth PH, Djukanovic R, Wilson J, Holgate ST, Roche WR (1990). Myofibroblasts and subepithelial fibrosis in bronchial asthma. Am J Respir Cell Mol Biol 3: 507–511.

Clevers H, Nusse R (2012). Wnt/β-catenin signaling and disease. Cell 149: 1192–1205.

Cohen ED, Ihida-Stansbury K, Lu MM, Panettieri RA, Jones PL, Morrisey EE (2009). Wnt signaling regulates smooth muscle precursor development in the mouse lung via a tenascin C/PDGFR pathway. J Clin Invest 119: 2538–2549.

Cokuğraş H, Akçakaya N, Seçkin İ, Camcioğlu Y, Sarimurat N, Aksoy F (2001). Ultrastructural examination of bronchial biopsy specimens from children with moderate asthma. Thorax 56: 25–29.

Curtis MJ, Bond RA, Spina D, Ahluwalia A, Alexander SPA, Giembycz MA *et al.* (2015). Experimental design and analysis and their reporting: new guidance for publication in BJP. Br J Pharmacol 172: 3461–3471.

Cutz E, Levison H, Cooper DM (1978). Ultrastructure of airways in children with asthma. Histopathology 2: 407–421.

De Langhe S, Carraro G, Tefft D, Li C, Xu X, Chai Y *et al.* (2008). Formation and differentiation of multiple mesenchymal lineages during lung development is regulated by beta-catenin signaling. PLoS One 3: e1516.

Eguchi M, Nguyen C, Lee SC, Kahn M (2005). ICG-001, a novel small molecule regulator of TCF/beta-catenin transcription. Med Chem Shāriqah United Arab Emir 1: 467–472.

Emami KH, Nguyen C, Ma H, Kim DH, Jeong KW, Eguchi M *et al.* (2004). A small molecule inhibitor of beta-catenin/CREB-binding protein transcription [corrected]. Proc Natl Acad Sci U S A 101: 12682–12687.

Flood-Page P, Menzies-Gow A, Phipps S, Ying S, Wangoo A, Ludwig MS *et al.* (2003). Anti-IL-5 treatment reduces deposition of ECM proteins in the bronchial subepithelial basement membrane of mild atopic asthmatics. J Clin Invest 112: 1029–1036.

Ghosh AK, Yuan W, Mori Y, Varga J (2000). Smad-dependent stimulation of type I collagen gene expression in human skin fibroblasts by TGF-beta involves functional cooperation with p300/CBP transcriptional coactivators. Oncogene 19: 3546–3555.

Ghosh AK, Yuan W, Mori Y, Chen S, Varga J (2001). Antagonistic regulation of type I collagen gene expression by interferon-gamma and transforming growth factor-beta. Integration at the level of p300/CBP transcriptional coactivators. J Biol Chem 276: 11041–11048.

Goodman RH, Smolik S (2000). CBP/p300 in cell growth, transformation, and development. Genes Dev 14: 1553–1577.

Gosens R, Stelmack G, Dueck G, McNeill K, Yamasaki A, Gerthoffer W *et al.* (2006). Role of caveolin-1 in p42/p44 MAP kinase activation and proliferation of human airway smooth muscle. Am J Physiol Lung Cell Mol Physiol 291: L523–L534.

Gosens R, Baarsma HA, Heijink IH, Oenema TA, Halayko AJ, Meurs H *et al.* (2010). De novo synthesis of {beta}-catenin via H-Ras and MEK regulates airway smooth muscle growth. FASEB J Off Publ Fed Am Soc Exp Biol 24: 757–768.

Hackett T-L, de Bruin HG, Shaheen F, van den Berge M, van Oosterhout AJ, Postma DS *et al.* (2013). Caveolin-1 controls airway epithelial barrier function. Implications for asthma. Am J Respir Cell Mol Biol 49: 662–671.

Hecht A, Vleminckx K, Stemmler MP, van Roy F, Kemler R (2000). The p300/CBP acetyltransferases function as transcriptional coactivators of beta-catenin in vertebrates. EMBO J 19: 1839–1850.

Heijink IH, Postma DS, Noordhoek JA, Broekema M, Kapus A (2010). House dust mite-promoted epithelial-to-mesenchymal transition in human bronchial epithelium. Am J Respir Cell Mol Biol 42: 69–79.

Henderson WR, Chi EY, Ye X, Nguyen C, Tien Y, Zhou B *et al.* (2010). Inhibition of Wnt/beta-catenin/CREB binding protein (CBP) signaling reverses pulmonary fibrosis. Proc Natl Acad Sci U S A 107: 14309–14314.

Horak E, Lanigan A, Roberts M, Welsh L, Wilson J, Carlin JB *et al.* (2003). Longitudinal study of childhood wheezy bronchitis and asthma: outcome at age 42. BMJ 326: 422–423.

Hoshino M, Nakamura Y, Sim J (1998). Expression of growth factors and remodelling of the airway wall in bronchial asthma. Thorax 53: 21–27.

Huang S-MA, Mishina YM, Liu S, Cheung A, Stegmeier F, Michaud GA *et al.* (2009). Tankyrase inhibition stabilizes axin and antagonizes Wnt signalling. Nature 461: 614–620.

Humbles AA, Lloyd CM, McMillan SJ, Friend DS, Xanthou G, McKenna EE *et al.* (2004). A critical role for eosinophils in allergic airways remodeling. Science 305: 1776–1779.

James AL, Bai TR, Mauad T, Abramson MJ, Dolhnikoff M, McKay KO *et al.* (2009). Airway smooth muscle thickness in asthma is related to severity but not duration of asthma. Eur Respir J 34: 1040–1045.

Jenkins HA, Cool C, Szefler SJ, Covar R, Brugman S, Gelfand EW*et al.* (2003). Histopathology of severe childhood asthma: a case series. Chest 124: 32–41.

Johnson SR (2005). TIMP-1 in asthma: guilty by association. Thorax 60: 617–618.

Kilkenny C, Browne W, Cuthill IC, Emerson M, Altman DG (2010). Animal research: Reporting in vivo experiments: the ARRIVE guidelines. Br J Pharmacol 160: 1577–1579.

Königshoff M, Eickelberg O (2010). WNT signaling in lung disease: a failure or a regeneration signal? Am J Respir Cell Mol Biol 42: 21–31.

Kumawat K, Koopmans T, Gosens R (2014). β-catenin as a regulator and therapeutic target for asthmatic airway remodeling. Expert Opin Ther Targets 18: 1023–1034.

Ma H, Nguyen C, Lee K-S, Kahn M (2005). Differential roles for the coactivators CBP and p300 on TCF/beta-catenin-mediated survivin gene expression. Oncogene 24: 3619–3631.

McCrea PD, Gu D (2010). The catenin family at a glance. J Cell Sci 123: 637–642.

McGrath JC, Lilley E (2015). Implementing guidelines on reporting research using animals (ARRIVE etc.): new requirements for publication in BJP. Br J Pharmacol 172: 3189–3193.

Meerschaert J, Kelly EA, Mosher DF, Busse WW, Jarjour NN (1999). Segmental antigen challenge increases fibronectin in bronchoalveolar lavage fluid. Am J Respir Crit Care Med 159: 619–625.

Melgert BN, Timens W, Kerstjens HA, Geerlings M, Luinge MA, Schouten JP *et al.* (2007). Effects of 4 months of smoking in mice with ovalbumin-induced airway inflammation. Clin Exp Allergy J Br Soc Allergy Clin Immunol 37: 1798–1808.

Metcalfe C, Bienz M (2011). Inhibition of GSK3 by Wnt signalling--two contrasting models. J Cell Sci 124: 3537–3544.

Meurs H, Gosens R, Zaagsma J (2008). Airway hyperresponsiveness in asthma: lessons from in vitro model systems and animal models. Eur Respir J 32: 487–502.

Miyabayashi T, Teo J-L, Yamamoto M, McMillan M, Nguyen C, Kahn M (2007). Wnt/beta-catenin/CBP signaling maintains long-term murine embryonic stem cell pluripotency. Proc Natl Acad Sci U S A 104: 5668–5673.

Mucenski ML, Nation JM, Thitoff AR, Besnard V, Xu Y, Wert SE *et al.* (2005). Beta-catenin regulates differentiation of respiratory epithelial cells in vivo. Am J Physiol Lung Cell Mol Physiol 289: L971–L979.

Nials AT, Uddin S (2008). Mouse models of allergic asthma: acute and chronic allergen challenge. Dis Model Mech 1: 213–220.

Nunes R, Schmidt M, Dueck G, Baarsma H, Halayko A, Kerstjens H *et al.* (2008). GSK-3/beta-catenin signaling axis in airway smooth muscle: role in mitogenic signaling. Am J Physiol Lung Cell Mol Physiol 294: L1110–L1118.

Oenema TA, Mensink G, Smedinga L, Halayko AJ, Zaagsma J, Meurs H *et al.* (2013). Cross-talk between transforming growth factor-β and muscarinic M receptors augments airway smooth muscle proliferation. Am J Respir Cell Mol Biol 49: 18–27.

Payne DNR, Rogers AV, Adelroth E, Bandi V, Guntupalli KK, Bush A *et al.* (2003). Early thickening of the reticular basement membrane in children with difficult asthma. Am J Respir Crit Care Med 167: 78–82.

Regamey N, Hilliard TN, Saglani S, Zhu J, Scallan M, Balfour-Lynn IM *et al.* (2007). Quality, size, and composition of pediatric endobronchial biopsies in cystic fibrosis. Chest 131: 1710–1717.

Ruijter JM, Ramakers C, Hoogaars WMH, Karlen Y, Bakker O, van den Hoff MJB *et al.* (2009). Amplification efficiency: linking baseline and bias in the analysis of quantitative PCR data. Nucleic Acids Res 37: e45.

Ruijter JM, Pfaffl MW, Zhao S, Spiess AN, Boggy G, Blom J *et al.* (2013). Evaluation of qPCR curve analysis methods for reliable biomarker discovery: bias, resolution, precision, and implications. Methods 59: 32–46.

Sears MR, Greene JM, Willan AR, Wiecek EM, Taylor DR, Flannery EM *et al.* (2003). A longitudinal, population-based, cohort study of childhood asthma followed to adulthood. N Engl J Med 349: 1414–1422.

Southan C, Sharman JL, Benson HE, Faccenda E, Pawson AJ, Alexander SP *et al.* (2016). The IUPHAR/BPS Guide to PHARMACOLOGY in 2016: towards curated quantitative interactions between 1300 protein targets and 6000 ligands. Nucl. Acids Res. 44: D1054–D1068.

Takemaru KI, Moon RT (2000). The transcriptional coactivator CBP interacts with beta-catenin to activate gene expression. J Cell Biol 149: 249–254.

Temelkovski J, Hogan SP, Shepherd DP, Foster PS, Kumar RK (1998). An improved murine model of asthma: selective airway inflammation, epithelial lesions and increased methacholine responsiveness following chronic exposure to aerosolised allergen. Thorax 53: 849–856.

Ulsamer A, Wei Y, Kim KK, Tan K, Wheeler S, Xi Y *et al.* (2012). Axin pathway activity regulates in vivo pY654-β-catenin accumulation and pulmonary fibrosis. J Biol Chem 287: 5164–5172.

Valenta T, Hausmann G, Basler K (2012). The many faces and functions of β-catenin. EMBO J 31: 2714–2736.

Volckaert T, Dill E, Campbell A, Tiozzo C, Majka S, Bellusci S *et al.* (2011). Parabronchial smooth muscle constitutes an airway epithelial stem cell niche in the mouse lung after injury. J Clin Invest 121: 4409–4419.

WHO (2013). Asthma. Available at: www.who.int/respiratory/asthma/en (accessed 11/1/2013).

Zwaenepoel K, Louis JV, Goris J, Janssens V (2008). Diversity in genomic organisation, developmental regulation and distribution of the murine PR72/B″ subunits of protein phosphatase 2 A. BMC Genomics 9: 393.